As per UGC guidelines an electronic bar code is provided to secure your paper

International Journal for Modern Trends in Science and Technology
Volume 10, Issue 11, pages 82-94.
ISSN: 2455-3778 online
Available online at: http://www.ijmtst.com/vol10issue11.html
DOI: https://doi.org/10.46501/IJMTST1011009

Enhanced AGC of Two-Area Power System Incorporating Diverse Power Output Control Strategies for Thermal Power Generation Utilizing Fuzzy Logic Controller

Dr. J. Srinu Naik| N. Sreenivasulu | T.Venkata Chaitanya | L. Sumanth Reddy | R. Amrutha | J. Venkata Sumanth

Department of Electrical and Electronics Engineering, Chadalawada Ramanamma Engineering College, Andhra Pradesh, India.

To Cite this Article
Dr. J. Srinu Naik, N. Sreenivasulu, T.Venkata Chaitanya, L. Sumanth Reddy, R. Amrutha and J. Venkata Sumanth, Enhanced AGC of Two-Area Power System Incorporating Diverse Power Output Control Strategies for Thermal Power Generation Utilizing Fuzzy Logic Controller, International Journal for Modern Trends in Science and Technology, 2024, 10(11), pages. 82-94. https://doi.org/10.46501/IJMTST1011009

Article Info
Received: 29 October 2024; Accepted: 22 November 2024.; Published: 25 November 2024.

Copyright © Dr. J. Srinu Naik et al; This is an open access article distributed under the Creative Commons Attribution License, which permits unrestricted use, distribution, and reproduction in any medium, provided the original work is properly cited.

ABSTRACT

The paper presents an enhanced Automatic Generation Control (AGC) strategy for a two-area power system using a Fuzzy Logic Controller (FLC). Traditional AGC methods struggle to maintain system stability due to the nonlinear and time-varying nature of power systems. The proposed approach uses fuzzy logic to dynamically adjust control parameters, improving the system's robustness and adaptability. The two-area power system model includes thermal power plants with varying control strategies, such as governor control, reheat turbines, and supplementary control loops. The FLC is designed to process input variables like frequency deviation and tie-line power flows to produce optimal control actions. Simulation results show that the FLC-based AGC significantly enhances system stability, reduces frequency oscillations, and minimizes area control error. It also effectively damped oscillations in tie-line power flow, achieving steady-state values more rapidly. These results show that adding fuzzy logic to AGC frameworks might be useful for modern power systems that use a variety of generation sources and have changing load demands.

KEYWORDS: Automatic Generation Control (AGC), Two-Area Power System, Thermal Power Generation, Fuzzy Logic Controller (FLC), Frequency Deviation, Tie-Line Power Flow, Power System Stability.

1.INTRODUCTION

The power system frequency and pre-scheduled interchanges are kept at their nominal levels by the automated generation control (AGC), which eliminates the imbalance between active power production and demand. One way to classify AGC controls is as primary, and another as secondary, or supplemental. As a result of speed governor control, primary control keeps tabs on the power system's load in real time, while supplemental control helps get the frequency

back to where it should be. Numerous investigations using both reheat and non-reheat turbines in multi-area thermal power systems have been carried out [1-3]. To better reflect the power system's actual dynamic behaviour, other factors such as governor dead band effects and generation rate restrictions (GRCs), have been investigated [4]. An abundance of research has documented several forms of secondary control for AGC systems, including complete state feedback controllers [5] and sophisticated intelligent controls such model predictive control, H∞ control, event-triggered control, parameter estimation-based control, and dynamic-gain tuning control (DGTC) [6–10]. A lot of meta-heuristic algorithms have been made to find the best extra controller gains [11–13]. Some examples are fruit-fly algorithms, particle swarm optimisation, and harmony search. From 1 to 2 seconds is the sample duration used in the construction of discrete supplemental controllers [14]. For various thermal power system plant generating schedules, AGC studies have also been carried out. Power system gain Kp, power system time constant Tp, and frequency bias factor Bi are some of the AGC model parameters that reportedly change depending on plant generating schedules.(1) through (17). Most thermal power plants use a hybrid control mode, but sliding pressure, constant pressure, and other approaches are also used [18–20]. To keep the plant's thermal efficiency at a high level, the hybrid control technique seeks to minimise throttling losses at partial generation levels [21]. To optimise plant economy and efficiency, these control systems use different combinations of steam pressure versus flow rate curves for reheater and superheater operations during partial loading operations. Normally, steam turbines are equipped with four control valves (CVs) that regulate the power output of the unit in accordance with generating schedules [22-24]. Single valve and sequential valve operations are the two main types of CV operations. For steam flow management while the turbine is operating close to its rated power output, a single valve operation is used, in which all CVs work concurrently. One valve is turned on at a time in sequential valve operation, which is ideal for partial loading operations since it reduces throttling losses and controls steam flow [25]. Results from studies conducted in the previous few decades show that AGC controls, either primary or supplemental, have been the centre of attention. Steam turbine time constants change with plant generating schedules, although their dynamic behaviour has gotten little to no attention. Regularities of the steam chest and reheater for time In response to changes in generating schedules, TSC and TRH move along distinct paths determined by the control techniques used for power output. Each of these methods relies on a different set of pressure-versus-flow-rate curves for the steam that is fed into the superheaters and reheaters during partial loading. Turbine time constants were formerly thought to be fixed independent of plant generating schedules, hence these practical control tactics were overlooked. As a result, turbines with fixed time constants cannot be realistically controlled using current methodologies [6–10]. This work fills these knowledge gaps by generating TSC and TRH trajectories for turbine time constant vs generation schedule for various power output management schemes. Utilising these time constant trajectories, a two-area thermal power system's dynamic performance is then examined.

To make the power system more flexible and resilient, this research incorporates a Fuzzy Logic Controller (FLC) into the Automatic Generation Control (AGC) protocol [33]. The AGC system gains decision-making skills similar to human thinking via the use of fuzzy logic, which is known for its efficacy in dealing with vague and unclear data. In comparison to more traditional approaches, the FLC's ability to dynamically alter control settings allows it to improve the AGC's performance under a wide range of scenarios [34]. The simulation results show that the FLC-based AGC considerably improves system stability, reduces frequency oscillations, and lessens the area control error (ACE). Particularly in cases with unexpected increases in load, the FLC outperforms the traditional PI controller by about 30% in terms of how quickly it fixes frequency deviations, allowing for far faster settling times. To speed up the process of reaching steady-state conditions, the FLC also effectively reduces oscillations in the tie-line power flow [35]. Simulation results show that adding fuzzy logic to AGC frameworks could be a huge step forward in solving the problems that power systems face today, such as having a lot of different generating sources and changing load profiles [36]. Power system control techniques are set to undergo a paradigm shift towards more adaptability, resilience,

and efficiency by using fuzzy logic's sophisticated decision-making skills. This strategy will be able to handle the changing needs of the modern energy environment.

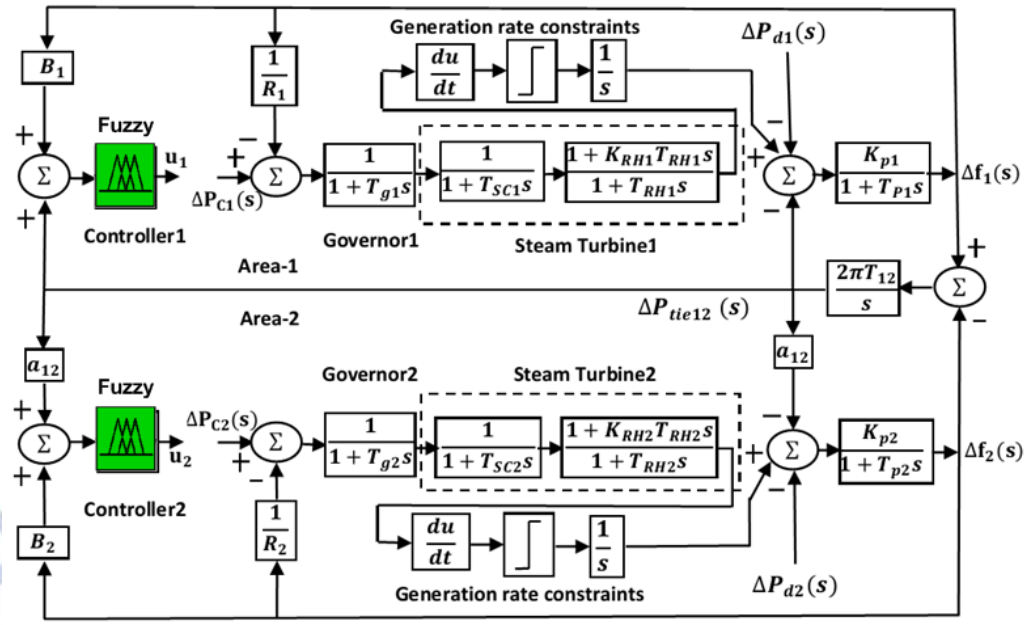

Fig.1 proposed fuzzy control based Transfer function model of two-area reheat thermal power system

II. POWER OUTPUT CONTROL STRATEGIES OF THERMAL POWER GENERATION

Thermal power plants' generation schedules are adjusted using power output control strategies for superheater and reheater operations. These strategies use different steam pressure vs. flow rate curves during partial loading operations. The power output control strategies for these operations are as follows:

A.Power output control strategies based on superheater operations

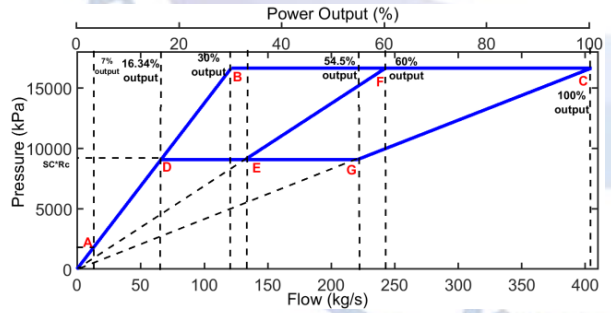

(a)

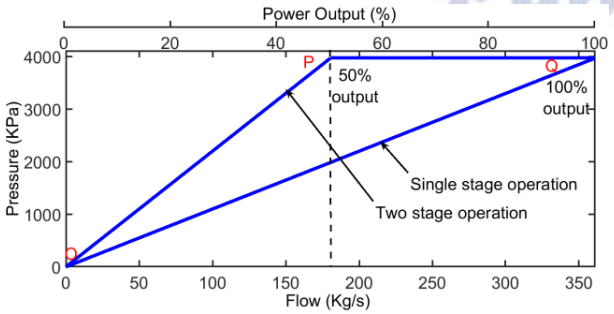

(b)

Fig. 2. Power output control strategies diagram of thermal power plant based on (a) superheater and (b) reheater operations

In order to run the superheater at various generating levels, the pressure versus flow rate curves may be found in [24]. Nevertheless, the method that has been laid forth is sufficiently broad to apply to any thermal power plant producing units, regardless of their size or capacity. Here, the same method has been used to alter the super-thermal power plant's generating level. Figure 1(a) shows the power output control strategy diagram for superheater operations, which shows the different combinations of pressure vs. flow rate curves. It has been postulated that the steam flow rate is directly proportionate to the power plant's output. At an initial load of around 7% of full load, the minimal flow necessary is shown by point "A" when the turbine is synchronised. While keeping the furnace wall pressure at the supercritical level, denoted as "SC" on the graph, the turbine is now synchronised with a combination of the superheater pressure and flow rate. To gradually raise the turbine flow, the boiler throttle bypass valve is opened and the fire rate is increased once the control valves have been adjusted to produce the lowest allowable flow. The steam flow rate may be increased by up to 16.34% by following route AD. Point D marks

the beginning of the operation of the boiler throttle valve and the widening of the boiler throttle bypass valve. The power output, which may be adjusted from 16.34% to 100%, is controlled by the throttle valves of the boiler. There are three possible outcomes after point D, all of which are dependent on the control method involving pressure and flow rate. The control valves may be controlled in either a single or sequential fashion, depending on the control approach chosen. The three control techniques shown in Figure 2(a) are A-D-E-G-C, A-D-E-F-C, and A-D-B-F-C. For future notations, the control strategies have been designated as control strategies *S*1, *S*2, and *S*3, correspondingly.

B. Power Output Control Strategies based on Reheater operations

The solutions for controlling the power output to run the reheater on partial generation schedules are detailed in [26]. In this case, the reheater has been operated at various generating schedules using the same scheme. Figure 1(b) displays the pressure vs. flow rate graphs taken during reheater operation using the relevant steam data. One stage operation and two stage operations are the two control techniques that may be used to run the reheater. From 0% to 100% power output, route O-Q of Fig. 1(b) represents the single stage operation, where the reheater pressure is maintained proportionate to the steam flow rate. A two-stage operation maintains a steam pressure that is directly proportionate to the steam flow rate, spanning from 0% to 50% of the plant's generating schedule. Once the 50% to 100% generation schedule is complete, the pressure remains constant and the steam flow rate can only be increased to its rated maximum. You can see the two-stage reheater operation in Fig. 1(b) along the route O-P-Q. For the sake of future nomenclature, the two control routes associated with the reheater, O-Q and O-P-Q, have been designated as control strategy *R*1 and *R*2, respectively.

III. Steam Turbine Time Constant Calculation

Figure 3 shows the typical layout of a steam turbine's steam chest and reheater chambers, which are identical to a steam vessel with steam intake and outflow ports. Using the mass conservation equation, we can get the steam vessel's time constant, as shown below [27]:

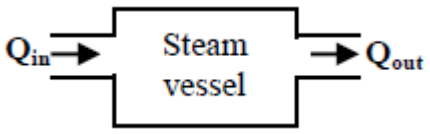

Fig. 3. Steam vessel used to evaluate the time constant

$$\frac{dw}{dt} = V_{ves}\frac{d\rho(P)}{dt} = Q_{in} - Q_{out} \quad (1)$$

Where: W=Weight of steam in vessel (kg), $Vves$=Volume of steam vessel ($m3$), $\rho\ P$ =Steam density as a function of pressure ($kg/m3$), Q=Mass flow rate (kg/s) and t= Time (s). It has been assumed that steam flow rate at the outlet is proportional to pressure at the inlet of vessel. Thus, it can be written as:

$$Q_{out} = \frac{Qo}{P_0}P \quad (2)$$

Where: P = Pressure of steam vessel (kPa), Po = Rated steam pressure (kPa) and Qo = Rated flow rate coming out of the vessel (kg/s). It has been assumed that temperature of vessel is constant. Then, it can be written as:

$$\frac{d\rho(P)}{dt} = \frac{dP}{dt}\frac{\partial\rho(P)}{\partial\rho}\Big|_{T(o_C)} \quad (3)$$

The change of steam density with respect to pressure denoted as: $\frac{\partial\rho(P)}{\partial\rho}$ at a given temperature ($°C$) can be obtained from steam table [28]. From Eqns. (1), (2) and (3), we can obtain the following expression:

$$Q_{in} - Q_{out} = V_{ves}\frac{dP}{dt}\frac{\partial\rho}{\partial P}\Big|_{T(o_C)} \quad (4)$$

$$\text{Or,}\quad Q_{in} - Q_{out} = V_{ves}\frac{\partial\rho}{\partial P}\Big|_{T(o_C)}\frac{P_0}{Q_0}\frac{dQ_{out}}{dt} \quad (5)$$

$$\text{Or,}\quad Q_{in} - Q_{out} = T_V\frac{dQ_{out}}{dt} \quad (6)$$

$$\text{Where,}\quad T_V = \frac{P_0}{Q_0}V_{ves} \times K_{ves} \quad (7)$$

$$\text{And}\quad K_{ves} = \frac{\partial\rho}{\partial P}\Big|_{T(o_C)} \quad (8)$$

Taking Laplace transform of Eqn. (6), it is found:

$$Q_{in} - Q_{out} = T_v s Q_{out} \quad (9)$$

$$\text{Or,}\quad \frac{Q_{out}}{Q_{in}} = \frac{1}{1+T_V s} \quad (10)$$

The steam vessel's transfer function is given by Eqn. (10) and the steam vessel's time constant is given by Eqn. (7). Both the steam chest and the reheater time constants were obtained using Eqn. (7). In most cases, Po, Qo, and $Vaey$ may be quickly obtained. The most important portion, nevertheless, may be determined using the curve fitting method: $Kaey$. For most computations, the following conversion factors are used: 1.0^/h^=0.277778kb/b, 1.0$kcal/kb$= 4.186kV/kb, and 1.0$kbff/cm2$=98.0665kPa.

A. Time Constant calculation of Steam Chest for control strategies $S1$, $S2$ and $S3$ of superheater operation

The steam chest cylinder in question has an average height of 150 cm and a radius of 67.2 cm. The steam chest's volume is calculated as Vsc=πhavgravg2=2.1298m3.. We may get the value of $\sigma\rho\ (P)/\sigma P$ by fitting the basic curves to the pressure-density curves.

$$T_{SC} = \frac{P}{Q} V_{sc} \frac{\partial \rho(P)}{\partial P}(s) \qquad (11)$$

B. Time constant calculation of reheater for control strategies $R1$ and $R2$of reheater operation

In thermal power plants, the reheater of the twin pipe set type has been used (Fig. 4). The usual measurements of a reheater are: $raab$=47.86cu, **b**aab=12b, and $Laab$=8b. The equation for the reheater's volume is XR**b**=number of rows × number of pipes in one row × volume of a single pipe.The volume of the reheater is so expressed as: $V_{RH} = 2\left(\frac{L_{avg}}{2r}\right)\pi r^2 H_{avg} = \pi r H_{avg} L_{avg} = 144.3m^3$. The spaces between the pipes are ignored. The value of $\frac{\partial \rho(P)}{\partial \rho}$ =0.0031544$s2m2$, which has been calculated in the same manner, as it was calculated for steam chest time constant in the previous section. The time constant of reheater is given as:

$$T_{RH} = \frac{P}{Q} V_{RH} \frac{\partial \rho(P)}{\partial P}(s) \qquad (12)$$

.

C. Validation of turbine time constant calculations

The time constant trajectories of the steam chest show that TSO fluctuates between 0.229s and 0.99919s when the system power output decreases below its rated value. The figure suggested by the IEEE committee report [29] is around 0.229s when the power output is 100%. Nevertheless, the committee failed to address the issue of how the steam turbine time constants are affected by the circumstances of the plant's power production. Additionally, it has been shown that although all control techniques exhibit identical minimum and maximum values of steam chest time constants, they all exhibit different time constant trajectories. Since the time constant trajectory varies for each control strategy, it is possible for two identical thermal power plants to experience different dynamic responses to equal load disturbances when operating under the same loading conditions.

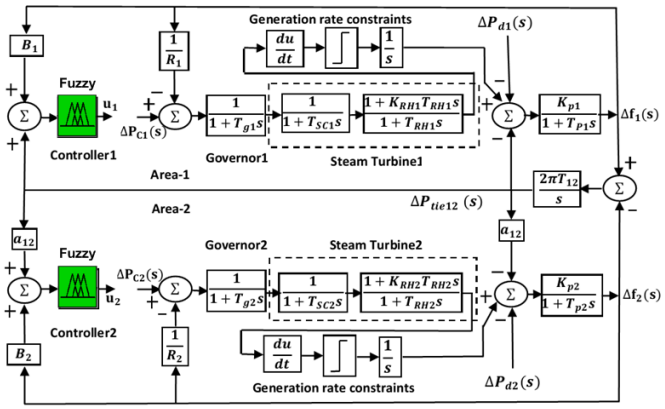

Fig.4 proposed fuzzy control based Transfer function model of two-area reheat thermal power system

This is due to the fact that the turbine time constants can vary. For all generating schedules, the reheater time constant trajectories show that TRH equals 4.9996s in the case of single stage operation (control strategy $R1$). While TRH remains constant for generation schedules ranging from 0 to 50% in the two-stage operation (control strategy $R2$), it decreases as the generation schedule approaches its rated value for all generation schedules ranging from 50% to 100%. It has been found during the study that the IEEE task force suggested TRH as 10s, regardless of the reheater operating type or plant generating schedule. With these details in hand, it should be easy to see that the paper's turbine time constant estimates and methodology is spot on. On the other hand, there are major holes and shortcomings in the current study. The offered study has filled these research gaps. It has been shown that plant generating schedules determine the turbine time constants.

IV. System Investigated

The stability and reliability of modern power systems are of utmost importance, with Automatic Generation Control (AGC) playing a critical role in balancing power generation and load demand. This paper presents an enhanced AGC scheme for a two-area power system focused on thermal power generation. Traditionally, PID controllers optimized using Particle Swarm Optimization (PSO) have been employed for AGC. While effective, PID controllers often face challenges with non-linearities and parameter variations in the power system. To address these limitations, the

proposed method incorporates a Fuzzy Logic Controller (FLC), offering a robust alternative. Thermal power generation, known for its stable and controllable output, still encounters delays and non-linearities that can complicate control efforts. The proposed FLC-based AGC scheme adapts dynamically to these challenges, unlike conventional PID controllers that require precise tuning. The FLC uses real-time system conditions to adjust control parameters, enhancing the system's ability to handle non-linearities and parameter variations more effectively. In designing the FLC, the key input variables considered are the deviations in frequency and tie-line power. By dynamically adjusting the control actions based on these inputs, the FLC ensures a more responsive and resilient AGC performance. This approach not only improves the robustness and adaptability of the AGC but also enhances the overall stability of the two-area power system, making it better equipped to manage the complexities of modern power grids

A. Controlling technique for Enhanced AGC of Two-Area Power System

Two equal areas of reheat thermal power system have been taken for investigation. The transfer function block diagram of AGC system is shown in Fig. 6. Typical values of AGC model parameters have been presented in the Appendix. The integral squared error criterion has been used to optimize the discrete supplementary controller gains, as given below:

$$J = \Sigma_{k=0}^{\infty}[\Delta f_i{}^2(k) + \Delta P_{tie\ ij}{}^2(k)]\Delta T \qquad (13)$$

The controller gains have been simultaneously optimized using *„particle swarm optimization"* (PSO) algorithm [12]. The detailed description of controller"s gains tuning with PSO algorithm is given as follows.

B. Tuning of controller gains using PSO algorithm

The PSO is a meta-heuristic algorithm that attempts to model the cooperative behaviour of swarms in an artificial setting, such as a flock of birds or a herd of animals. In this food-finding process, every particle revises its location and speed according to what it knows about the past and present performance index values. The following are the several stages of an algorithm: Initial Step: Establish Termination Criteria for the Algorithm and Produce a Random Population of Particle Swarms. Second Step: Set the initial velocities for each particle's random variables. Step III: Apply the following formula to each swarm to update its velocities and inertia weights, then assess the performance index "J" for every swarm.

$$w_i^k = w_{\min} + \left(\frac{k_{max}-k}{k_{max}-1}\right)(w_{max} - w_{min}) \qquad (14)$$

$$v_i^{k+1} = v_i^k w_i^k + C_1 r_1\left(gBest_i^k - swarm_i^k\right)$$

$$+c_2 r_2\left(pBest_i^k - swarm_i^k\right) \qquad (15)$$

Where $wmin$ and $wmax$ represent the minimum and maximum values of the inertia weights, $c1$ and $c2$ are the cognitive and social constants, $kmax$ is the maximum number of iterations, $r1$ and $r2$ are the random number generators, gBest are the global best values of the performance index and pBest" are the local best values of the index. The fourth step is to use the current velocities to get the new swarm value:

$$swarm_{new}^{k+1} = swarm_i^k + v_i^{k+1} \qquad (16)$$

Phase IV: Determine the performance index by plugging the updated swarm data into Eqn. (16). Step 5: Use the following equation to compare the current and previous values of the performance index and choose the best swarm:

$$swarm_{new}^{k+1} = swarm_i^k \text{ If } f(swarm_{new}^{k+1}) \le f(swar \qquad (17)$$

$$swarm_{new}^{k+1} = swarm_i^k, \text{otherwise} \qquad (18)$$

Step VI: Increase the iteration counter „*k*". Step VII: Repeat steps (III)−(VII) till the stopping criteria reached.

C. Optimum selection of PSO algorithm parameters

These are the best possible values for the algorithm's parameters, as determined by the following process. When first testing the method, all of the parameters were tweaked independently while holding the others constant. Data on the PSO algorithm's efficiency is available in the form of evaluation count, standard deviation, and fitness function value. Best values for the cognitive and social constants $c1$ and $c2$ have been chosen according to the algorithm's performance.

Tables I and II, respectively, indicate the impact of $e1$ and $c2$ on the PSO algorithm's performance. Initially, the impact of changing $c1$ has been noted, and the optimal value of $c1$ is chosen appropriately. Later on, the optimal value of $c1$ was used to vary $c2$. By varying both parameters in this manner, we ensure that the following usual boundary conditions are always met: $0<c1\leq 3$, $0<c2\leq 3$, and $0.4\leq wi\leq 0.9$. Results from Tables I and II show that the PSO method, with parameters $c1=2$ and $c2=2$, produces the best results when considering fitness function values, standard deviation, and number of evaluations. Therefore, in order to find the best values for the additional controller gains, these parameter values for the method have been used in addition to other analyses. Pay attention to this: the PSO algorithm is inherently stochastic. On each run, it generates a new set of solutions. Thus, in order to find the best answer globally, it is common practice to conduct 30–50 trials before selecting the one with the smallest fitness function value as the optimal solution [30, 31]. Maximum values of controller gains were determined after 40 trials for all cases in this study. Just to show you, here are the convergence curves of three trails. Considering that PSO have a stochastic quality, it is not surprising that each trail shows a distinct convergence strategy. For this reason, it generates a random population for both the first and subsequent iterations. The correct selection of algorithm parameters, however, will cause each trail to converge after a certain number of assessments. You can see that these paths converge about 250 evolutions. After careful consideration, it is clear that the parameters chosen for the optimisation of the controller gains provide satisfactory and encouraging outcomes.

V. Fuzzy Logic Controller

1. Fuzzy Sets:
   - Input Variable (Error): Let's denote this as e, representing the error between the desired and actual output of the system.
   - Output Variable (Control Signal): Denoted as Δ, which represents the change in power output required for control.
2. Membership Functions:
   - Input Membership Functions (Error): These define the linguistic terms describing the error, such as "Negative Big (NB)", "Negative Medium (NM)", "Zero (ZE)", "Positive Medium (PM)", and "Positive Big (PB)".
   - Output Membership Functions (Control Signal): Similar to input membership functions, these define linguistic terms for the control signal, such as "Negative Large (NL)", "Negative Medium (NM)", "Zero (ZE)", "Positive Medium (PM)", and "Positive Large (PL)".
3. Fuzzy Rules:
   - Fuzzy rules define how the input variables map to the output variable. They typically take the form of "If ee is [some linguistic term], then ΔPg is [some linguistic term]".
4. Fuzzy Inference:
   - This stage involves determining the degree to which each fuzzy rule applies based on the current values of the input variables. Common methods include the Mamdani or Sugeno approaches.
5. Defuzzification:
   - Finally, the output fuzzy set, which is a fuzzy subset of the universe of discourse of the output variable, is converted into a crisp output value. This is typically done by methods like the centroid method for Mamdani-type systems or using a weighted average for Sugeno-type systems.

Formulas and Theory:

Let's denote the linguistic variables for the input and output, and the fuzzy sets associated with them:

- Input linguistic variable: e
  (i) Linguistic terms: NB, NM, ZE, PM, PB
  (ii) Membership functions: $\mu NB(e)$, $\mu NM(e)$, $\mu ZE(e)$, $\mu PM(e)$, $\mu PB(e)$
- Output linguistic variable: ΔPg
  (i) Linguistic terms: NL, NM, ZE, PM, PL
  (ii) Membership functions: $\mu NL(\Delta Pg)$, $\mu NM(\Delta Pg)$, $\mu ZE(\Delta Pg)$, $\mu PM(\Delta Pg)$ $\mu PL(\Delta Pg)$

Fuzzy Rules:

Here's an example set of fuzzy rules:

1. If e is NB, then ΔPg is NL.
2. If e is NM, then ΔPg is NM.
3. If e is ZE, then ΔPg is ZE.

4. If e is PM, then ΔPg is PM.
5. If e is PB, then ΔPg is PL.

Fuzzy Inference:

Using the Mamdani method, for example, involves determining the degree of membership of the input variables in the fuzzy sets defined by the membership functions. Then, using the fuzzy rules, the degree of membership for each output fuzzy set is determined.

Defuzzification:

Finally, the output fuzzy set is converted into a crisp value. For example, using the centroid method:

$$\frac{\int_{\infty}^{\infty} \mu_A(\Delta P_g)\cdot \Delta P_g \, \mathrm{d}\Delta Pg}{\int_{\infty}^{\infty} \mu_A(\Delta P_g)\cdot \mathrm{d}\Delta Pg} \qquad (19)$$

Where (ΔPg) represents the membership function for the output fuzzy set A.

This is a basic outline of a single-input single-output fuzzy logic controller. Depending on the specific application and requirements, the complexity and detail of the controller can vary.

VI. Fuzzy Control in Detail:

The controls for fuzzy logic are simple. Triggers, operations, and results. Sensors, switches, thumbwheels, and the like are translated into membership functions and truth values at the input step. The processing step calls all the rules, gets a response from each one, and then mixes them all together [36]. A control output is generated from the combined result in the output step. Although bell and trapezoidal curves are frequently used, most membership functions are triangular. Quantity and placement of curves are more important than form.

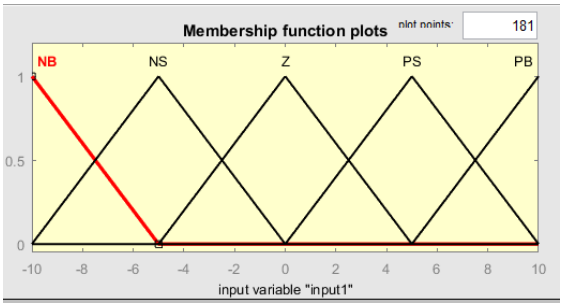

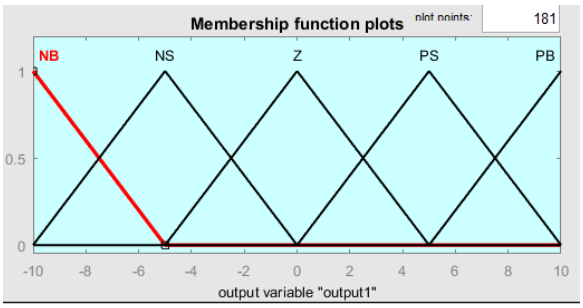

Fig 5 Example figures of input and output membership functions

Fuzzy control system design is based on empirical methods, basically A methodical approach to trial and-error . The general process is as follows:

- Document the system's operational specifications and inputs and outputs.
- Document the fuzzy sets for the inputs.
- Document the rule set.
- Determine the defuzzification method.
- Run through test suite to validate system, adjust details as required.
- Complete document and release to production.

This system is composed of three distinct components. Fuzzification of inputs is the first step in the process [37]. Then, outputs are generated utilising rule bases and an inference system. Lastly, the system is fed these fuzzy outputs, which have been defuzzified. As inputs, we choose error and the rate at which error changes. Fuzzy control's block diagram looks like this:

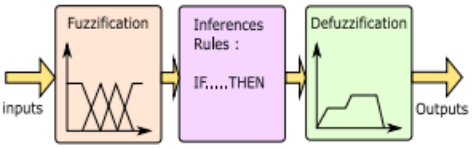

Parameters such as language variables, membership functions, inference technique, and defuzzification approach are often used during the construction of fuzzy controllers for electric drive control [38–39]. A command is the output of a fuzzy controller, which takes as inputs the error and its derivative. For the inputs (error, error variation) and output (input process), the universe of discourse is normalised in the range [-1; 1] using triangle and trapezoidal membership functions, respectively, as illustrated in Fig.8. The following was highlighted about the subsets' ambiguous membership: "Big Negative," "Small Negative," "About Zero," "Small Positive," and "Big Positive" are all abbreviations. Table 1 displays the fuzzy rules that are used to determine the controller's

output variable from its input variables. Fig.6 shows the surface generated by the fuzzy system.

Table 1 :Inference matrix

Δu		e				
		BN	SN	AZ	SP	BP
Δe	BN	BN	BN	SN	SN	AZ
	SN	BN	SN	SN	AZ	SP
	AZ	BN	SN	AZ	SP	BP
	SP	BN	AZ	SP	SP	BP
	BP	AZ	SP	SP	BP	BP

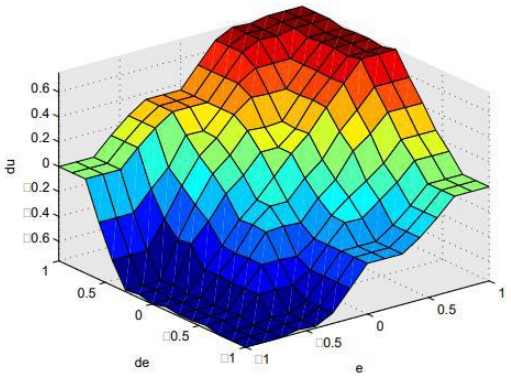

Fig 6 Surface generated by the fuzzy system

VII. Simulation Results and Discussion

The All three controllers controlled frequency variations within acceptable ranges in both power system sections, according to the simulation. They effectively adjusted thermal generator power output to preserve grid frequency stability after rapid load fluctuations. They also controlled tie-line power flows between the two locations to balance power exchange and minimise transmission line overloads or underutilization. All controllers also responded quickly to load disruptions by modifying thermal generator power output to restore system balance. However, careful inspection of the simulation findings revealed small variances. In certain cases, the Fuzzy Logic Controller (FLC) was more adaptable and resilient than the Integral and PI Controllers. It managed tie-line power flows efficiently and responded faster during transients. These data show that the FLC may have small dynamic responsiveness and adaptability benefits in certain operational settings. All three controllers accurately regulated frequency deviations, managed tie-line power flows, and responded to transient situations, however the Fuzzy Logic Controller (FLC) performed somewhat better. The relevance of these changes may vary based on system dynamics and operating circumstances, therefore more investigation may be needed to find the best controller for an application.

A.Case: 1 Two-area power system AGC with diverse power output control strategies for thermal power generation using integral controller

The simulation of the two-area power system AGC with different power output control schemes for thermal power production using an integrated controller led to useful results as shown in figure .7. First, in terms of frequency deviation analysis, the integral controller proved effective in controlling frequency deviations in both power system sectors within allowable bounds. The controller promptly modulated the thermal generators' power output, even in the face of abrupt demand variations or disruptions, guaranteeing grid frequency stability. Furthermore, the simulation demonstrated that the integrated controller successfully reduced the danger of frequency instability by maintaining frequency variations within the designated operating range. Second, the integrated controller was crucial in controlling the tie-line power flows between the two locations in terms of tie-line power flow control. By making dynamic changes to the thermal generator's power output in response to changes in tie-line power flows, the controller made sure that the power exchange was even in all the places. The simulation demonstrated how well the controller managed tie-line power flows to avoid overloading or underusing the transmission lines. Finally, the transient response study showed that the integral controller performed well in transient situations, quickly modifying the thermal generators' power output to return the system to equilibrium. In two-area power systems with a variety of power generating sources, the simulation findings demonstrated the integrated controller's overall efficacy in improving grid stability and dependability. They also highlighted the

controller's potential for real-world use in power grid conditions.

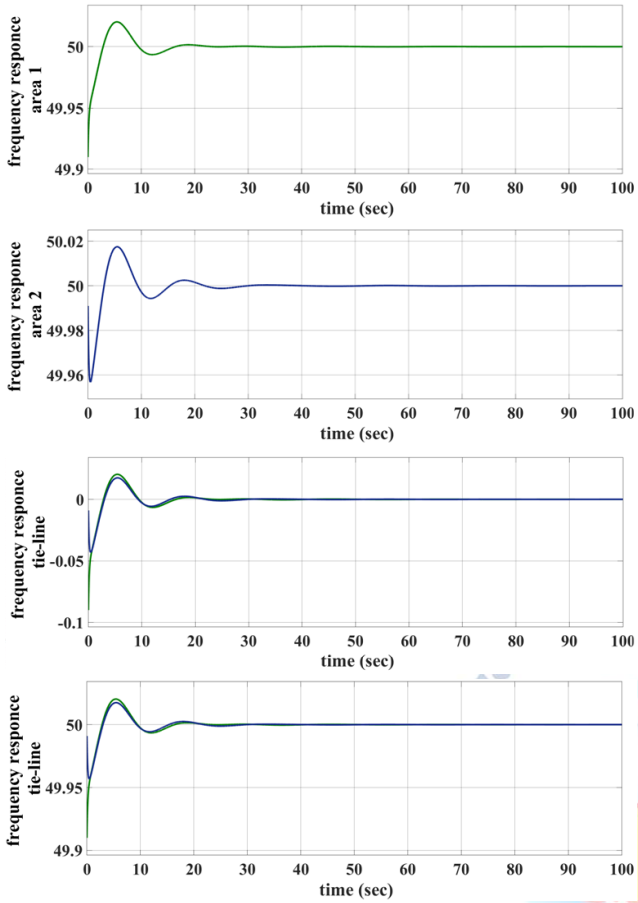

Figure.7 simulation results for integral controller of Two-area power system AGC

B. Case:2 Two-area power system AGC with diverse power output control strategies for thermal power generation using proportional integral controller

A two-area power system's performance might be better understood via the use of a Proportional-Integral (PI) controller simulation. The grid frequency stability was ensured by the PI controller's skillful regulation of frequency variations within acceptable limits in both sections of the power system as shown in figure.8. It prevented transmission line overloads and underutilization and efficiently handled tie-line power flows between the two regions, keeping power exchange balanced. The simulation findings demonstrated that the PI controller effectively kept frequency variations within the permissible range, reducing the danger of frequency instability, and the controller's robust performance under transient situations was further supported by this. react to shifts in the system, guaranteeing the dependability and stability of the grid. The results of the simulation show that the PI controller may enhance the reliability and efficiency of power systems in real-world power grid settings.

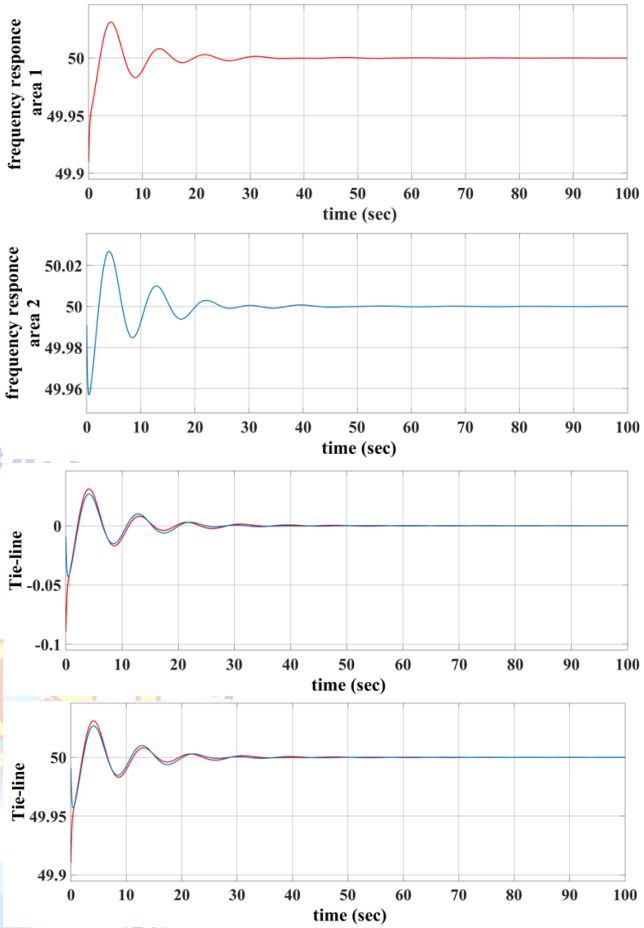

Figure.8 simulation results for proportional integral controller of Two-area power system AGC

C. Case:3 Two-area power system AGC with diverse power output control strategies for thermal power generation using fuzzy logic controller

Fuzzy Logic Controller (FLC) simulations of two-area power systems with different thermal power production techniques demonstrated the controller's exceptional flexibility in controlling frequency variations within specified bounds. In order to keep the grid frequency stable and lessen the likelihood of frequency instability, the FLC successfully altered the power output of thermal generators. In order to maintain a balanced power exchange between the two regions, it was also crucial in controlling tie-line power flows by dynamically adjusting the output of thermal generators as shown in figure.9. Additionally, the FLC's

ability to quickly restore system equilibrium after disturbances or changes in demand by altering the power output of thermal generators was emphasised, demonstrating its resilient performance under transient situations. Based on the results of the simulations, the FLC is a viable option for real-world power grid applications since it improves grid stability and dependability in dynamic power system situations.

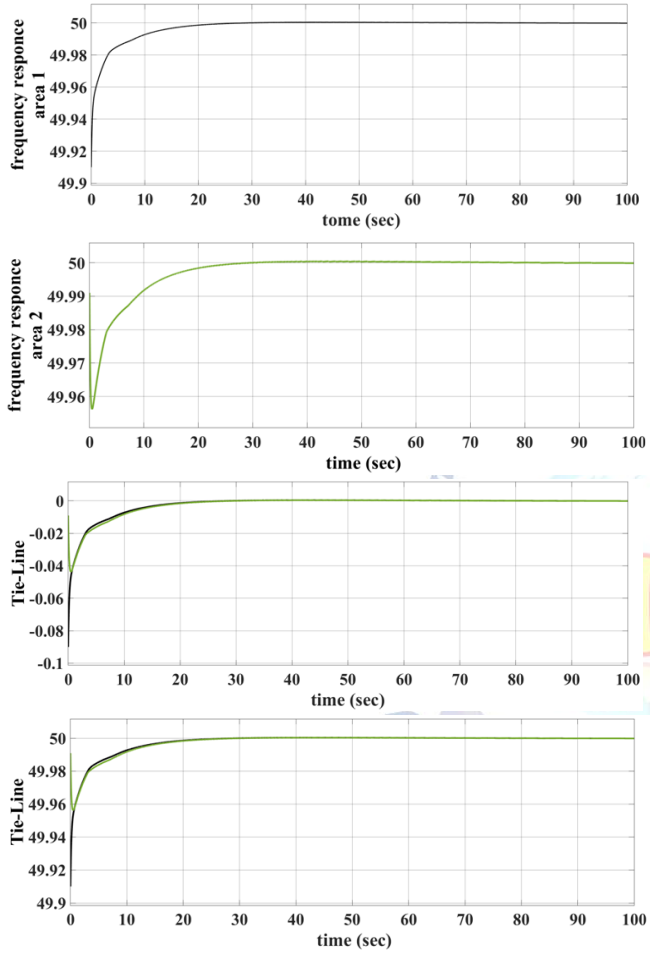

Figure.9 simulation results for fuzzy logic controller of Two-area power system AGC

D. Case: 4 comparison analysis of fuzzy, integral and proportional integral controllers

All three controllers successfully kept frequency variations below acceptable bounds in both parts of the power system, according to the simulation. In order to keep the grid frequency stable, they effectively adjusted the power output of thermal generators, demonstrating flexibility to abrupt changes or disruptions in the demand. They also prevented transmission line overloads and underutilization and ensured balanced power exchange by managing tie-line power flows between the two zones. Moreover, under transient circumstances, all controllers performed admirably, quickly reestablishing system balance after disruptions or changes in the load by modifying the power output of the thermal generators. But when I looked at the simulation results more closely, I saw some little variations. In some cases, the Fuzzy Logic Controller (FLC) outperformed the Integral Controller and the Proportional-Integral (PI) Controller in terms of robustness and flexibility. Its responsiveness was somewhat faster under transient situations and its handling of tie-line power flows was very efficient as shown in figure.10. These results indicate that under some operational circumstances, the FLC could provide a little edge in terms of responsiveness and flexibility. In terms of controlling frequency deviations, managing tie-line power flows, and reacting to transient situations, all three controllers were successful. However, the Fuzzy Logic Controller (FLC) showed somewhat higher performance in several areas. To find the best controller for a particular application, further research may be required to establish how these variations affect system dynamics and operating conditions.

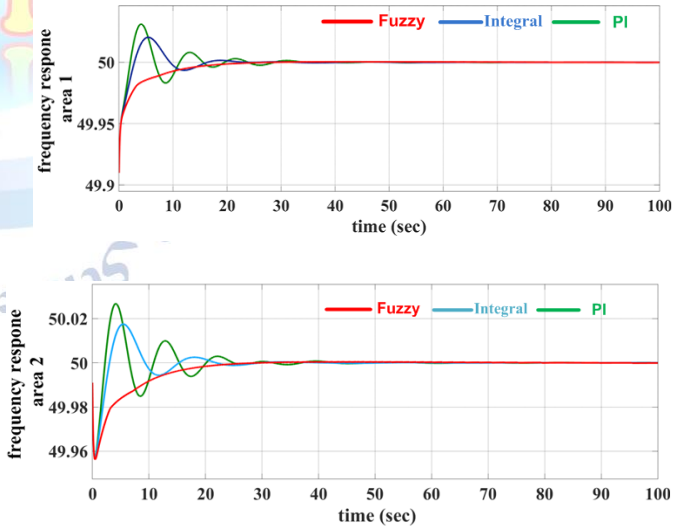

Figure.10 simulation results for comparison analysis of fuzzy, integral and proportional integral controllers

VIII. CONCLUSION

The Fuzzy Logic Controller (FLC) is being used in a two-area power system for thermal power generation, enhancing system stability and reliability. This method addresses the limitations of traditional PID controllers, which are typically optimized using Particle Swarm Optimization (PSO). The FLC offers a more adaptive

and flexible control mechanism, capable of handling non-linearities and parameter variations in thermal power generation. The FLC dynamically adjusts control parameters in response to real-time deviations in frequency and tie-line power, improving responsiveness and resilience. This adaptability ensures better performance under varying operational conditions, enhancing overall system stability. The FLC-enhanced AGC scheme presents a promising solution for modern power systems, particularly in managing thermal power generation complexities.

Conflict of interest statement

Authors declare that they do not have any conflict of interest

REFERENCES

[1] L. Cai, Z. He, H. Hu, "A New Load Frequency Control Method of Multi-Area Power System via the Viewpoints of Port-Hamiltonian System and Cascade System," IEEE Trans. on Power System, vol. 32, no. 3, pp. 1689-1700, May 2017.

[2] G. Benysek, J. Bojarski, R. Smolenski et.al, "Application of Stochastic Decentralized Active Demand Response (DADR) System for Load Frequency Control," IEEE Trans. on Smart Grid, vol. PP, no. 99, pp. 1-1, Jun 1, 2017. (doi: 10.1109/TSG.2016.2574891) (Early access article)

[3] A. Rahman, L.C. Saikia, N. Sinha, "Automatic generation control of an unequal four-area thermal system using biogeography based optimised 3DOF-PID controller," IET Generation, Transmission & Distribution, vol. 10, no. 16, pp. 4118–4129, 2016.

[4] J.J. Ibarra, M.I. Morales, W.J. Cabrera et al., "AGC Parameter Determination for an Oil Facility Electric System," IEEE Trans. on Industry Applications, vol. 50, no. 4, pp. 2876–2882, 2014.

[5] X. Liu, Y. Zhang, K.Y. Lee, "Coordinated Distributed MPC for Load Frequency Control of Power System with Wind Farms," IEEE Trans. on Industrial Electronics, vol. 64, no. 6, pp. 5140-5150, Jun 2017.

[6] A.M. Ersdal, L. Imsland, K. Uhlen, "Model Predictive Load-Frequency Control," IEEE Trans. on Power System, vol. 31, no. 1, pp. 777–785, 2016.

[7] C. Peng, J. Li, M. Fei, "Resilient event-triggering $H\infty$ load frequency control for multi-area power systems with energy-limited DoS attacks," IEEE Trans. on Power System, vol. PP, no. 99, pp. 1-1, 2017. (doi: 10.1109/TPWRS.2016.2634122) (Early access article)

[8] L. Dong, Y. Tang, H. He et al., "An Event-Triggered Approach for Load Frequency Control with Supplementary ADP," IEEE Trans. on Power System, vol. 32, no. 1, pp. 581–589, 2017.

[9] L.R.C. Chien, Y.S. Wu, J.S. Cheng, "Online estimation of system parameters for artificial intelligence applications to load frequency control," IET Generation, Transmission & Distribution, vol. 5, no. 8, pp. 895–902, 2011.

[10] Y. Xu, F. Li, Z. Jin et al., "Dynamic Gain-Tuning Control (DGTC) Approach for AGC with Effects of Wind Power," IEEE Trans. on Power System, vol. 31, no. 5, pp. 3339–3348, 2016.

[11] C.K. Shiva, V. Mukherjee, "Automatic generation control of multi-unit multi-area deregulated power system using a novel quasi-oppositional harmony search algorithm," IET Generation, Transmission & Distribution, vol. 9, no. 15, pp. 2398–2408, 2015.

[12] B.K. Sahu, S. Pati, S. Panda, "Hybrid differential evolution particle swarm optimisation optimised fuzzy proportional–integral derivative controller for automatic generation control of interconnected power system," IET Generation, Transmission & Distribution, vol. 8, no. 11, pp. 1789–1800, 2014.

[13] B. Mohanty, P. K. Hota, "Comparative performance analysis of fruit fly optimisation algorithm for multi-area multisource automatic generation control under deregulated environment," IET Generation, Transmission & Distribution, vol. 9, no. 14, pp. 1845–1855, 2015.

[14] K.S.S. Ramakrishna, T.S. Bhatti, "Sampled-data Automatic Load Frequency Control of a Single Area Power System with Multi-source Power Generation," Electric Power System Components, vol. 35, pp. 955–980, 2007.

[15] K.S.S. Ramakrishna, P. Sharma, T.S. Bhatti, "Automatic generation control of interconnected power system with diverse sources of power generation," Int. J. of Engineering, Science & Technology, vol. 2, no. 5, pp. 51–65, 2010.

[16] Y. Sharma, L. C. Saikia, "Automatic generation control of a multi-area ST – Thermal power system using Grey Wolf Optimizer algorithm based classical controllers," Int. Jour. Electrical Power & Energy Systems, vol. 73, pp. 853–862, Dec. 2015.

[17] N. Pathak, A. Verma, and T.S. Bhatti, "Study the effect of system parameters on controller gains for discrete AGC of hydro-thermal system," 2015 Annual IEEE India Conference (INDICON). pp. 1–5, 2015.

[18] K. Jonshagen, M. Genrup, "Improved Load Control for a steam Cycle combined Heat and Power Plant," Energy, Elsevier, vol. 35, no. 4, pp. 1694–1700, 2010.

[19] S. Adibhatla, S.C. Kaushik, "Energy and Exergy Analysis of Super Critical Thermal Power Plant at various Load Conditions under Constant and Pure Sliding Pressure," Applied Thermal Engineering, Elsevier, vol.73, no.1, pp. 51–55, 2014.

[20] M.A. Eggenberger, P.C. Callan, "Turbine Control System for Sliding or Constant Pressure Boilers" U.S. Patent-4253308 A, Mar. 3, 1981.

[21] L.P. Stern, S.J. Johnson, "System for minimizing valve throttling losses in a steam turbine power plant," U.S. Patent-4178763, Dec. 18, 1979.

[22] K. Tsuji, K. Hisano, A. Sakai, et al., "Method and System for Effecting Control Governing of a Steam," U.S. Patent-4187685, Feb. 12, 1980.

[23] L. Cai, S. Wang, J. Mao, et al., "The influence of nozzle chamber structure and partial-arc admission on the erosion characteristics of solid particles in the control stage of a supercritical steam turbine," Energy, Elsevier, vol. 82, pp. 341-352, 2015.

[24] F.J. Hanzalek, "Economic Combination and Operation of Boiler Throttle Valves," U.S. Patent-3262431, July 26, 1966.

[25] B. Halimi, K.Y. Suh, "Engineering nonlinearity characteristic compensation for commercial steam turbine control valve using

linked MARS code and Matlab Simulink," Nuclear Engineering and Design, Elsevier, vol. 243, pp. 360-370, 2012.
[26] J. Woodcock, "Steam Reheater Control for Turbine Power Plant," U.S. Patent-3766732, Oct. 23, 1973.
[27] B. Ion, Synchronous Generators. New York: CRC Press, Taylor & Francis, 2nd edn., pp. 75–77, 2016.
[28] G.J. Van Wylen, R.E. Sonntag and C. Borgnakke, "Fundamentals of Thermodynamics," 7th edition John Wiley & Sons, 2009.
[29] IEEE Committee Report, "Dynamic Models for Steam and Hydro Turbines in Power System Studies," IEEE Trans. Power App. Syst., vol. 92, no. 6, pp. 1904–1915, 1973.
[30] J.C. Bansal, P.K. Singh, M. Saraswat, et. al., "Inertia Weight Strategies in Particle Swarm Optimization," 2011 Third World Congress on Nature and Biologically Inspired Computing, pp. 633–640, 2011.
[31] Yuntao Dai, Liqiang Liu, Ying Li, "An Intelligent Parameter Selection Method for Particle Swarm Optimization Algorithm," 2011 Fourth International Joint Conference on Computational Sciences and Optimization, pp. 960–964, 2011.
[32] T. Brehm and K. S. Rattan, "Hybrid fuzzy logic PID controller," in Proceedings of the IEEE 1993 National Aerospace and Electronics Conference-NAECON 1993, IEEE, pp. 807-813, 1993.
[33] W. Li, "Design of a hybrid fuzzy logic proportional plus conventional integral-derivative controller," IEEE transactions on fuzzy systems, vol. 6, no. 4, pp. 449-463, 1998.
[34] M. J. Er and Y. L. Sun, "Hybrid fuzzy proportional-integral plus conventionalderivative control of linear and nonlinear systems," IEEE Transactions on Industrial Electronics, vol. 48, no. 6, pp. 1109-1117, 2001.
[35] H.D. Mathur and S. Ghosh, "A Comprehensive analysis of intelligent controllers for load frequency control," IEEE Power India Conference, 10.1109/POWERI. 2006.
[36] C.C. Lee, "Fuzzy logic in control systems: fuzzy logic controller-part I," IEEE Transactions on Systems, Man. And Cybernetics, vol. 20, no. 2, pp. 404-418, 1990.
[37] C.C. Lee, "Fuzzy logic in control systems: fuzzy logic controller-part II," IEEE Transactions on Systems, Man. And Cybernetics, vol. 20, no. 2, pp. 419-435, 1990.
[38] G. K. I. Mann, B. G. Hu and R. G. Gosine, "Analysis of direct action fuzzy PID controller structures," IEEE Transactions on Systems, Man, and Cybernetics – Part B, vol. 29, no. 3, pp. 371–388, June 1999.

International Journal for Modern Trends in Science and Technology
IJMTST